A Multi-Scale 3D Terrain Modeling and Visualization Method for Radiating Tidal Sand Ridges Based on DEM

Zhiming Wan¹, Xinyu Huang¹, Yuan Ding ^{1,2,*}

¹School of Earth Sciences and Engineering, Hohai University, Nanjing 211100, China

²College of Geography and Remote Sensing, Hohai University, Nanjing 211100, China

Keywords: Radiating sand ridges group, 3D terrain modeling, Semantic constraints, LOD, Tidal channel feature extraction.

Abstract

To address challenges in modeling radiating tidal sand ridge groups—such as weakened feature representation, insufficient semantic expression, and low visualization efficiency—this study proposes a "feature fusion–semantic constraint–spatial clustering" framework based on DEM data. A dual-window dynamic threshold model integrates a 9×9 relief window with a 3×3 coefficient of variation, enabling adaptive extraction of terrain features. Semantic constraints are introduced by using the D8 algorithm to extract tidal channels and constructing a constrained TIN, improving feature representation by 8.1% over the standard VIP method. A semantic-aware simplification mechanism assigns higher protection to major channels ($\lambda = 10$) and applies dynamic tolerance elsewhere, preserving morphological integrity at 96.86%. Furthermore, terrain zones are classified via landscape indices into core, transition, and background areas, supporting a three-level LOD strategy that enhances rendering efficiency while maintaining geometric fidelity in key regions. Cognitive evaluations confirm the method's superiority in visual clarity and structural accuracy, providing an effective solution for coastal terrain analysis and planning.

1. Introduction

1.1 General Instructions

Radiating tidal sand ridge groups are distinctive geomorphic units formed by the interaction of fluvial and marine dynamics. The system along the southern Yellow Sea, comprising over 70 interwoven sand ridges and tidal channels, contains rich terrestrial-derived sand resources and significant potential for deep-water port development. These land—sea transitional zones are critical for understanding environmental evolution and supporting sustainable coastal development in Jiangsu Province (Wang Y et al., 1999) .

Existing research has evolved from large-scale pattern analysis to investigations of local hydrodynamic mechanisms. For instance, Gu Yu et al. analyzed the system's evolution using remote sensing and GIS (Gu Yu et al., 2010), while Huachun H et al. assessed the Lanyang Sandbar's port potential based on sediment data and hydrodynamic modeling (Huachun H et al., 2005). However, most studies still rely on traditional 2D remote sensing imagery or numerical simulations, limiting the ability to quantify complex 3D terrain features such as elevation-induced feedback mechanisms. Furthermore, current models prioritize geometric representation while neglecting semantic terrain attributes.

3D terrain modeling and simplification are fundamental to digital terrain analysis. TIN models based on Delaunay triangulation—known for their circumscribed circle and minimum-angle maximization properties—are widely used. Parallel computing methods and GPS-aligned photogrammetry models have improved reconstruction efficiency. However, regular-grid DEM-based 3D modeling often loses microtopographic features during simplification. Traditional global optimization-based TIN algorithms lack real-time adaptability, and QEM-based simplification methods may fail to preserve

semantic features due to their vertex clustering nature. While edge folding algorithms like Hoppe H et al.'s prioritize low-distortion geometry, they rely on single-error metrics, resulting in the homogenization of terrain semantics (Hoppe H et al., 1993).

Multi-scale 3D modeling improves both performance and perception by adjusting detail levels based on viewpoint distance. Static and dynamic LOD strategies balance visual quality and rendering efficiency but rarely account for spatial heterogeneity. Du Y proposed integrating TIN and mipmap textures for hierarchical modeling (Du Y, 2005), yet most LOD approaches remain graphics-driven, with limited geographic dimensional expression.

To address these limitations, this study proposes a high-precision multi-scale terrain modeling framework based on adaptive TINs derived from DEM data. It ensures both geometric and semantic feature preservation, surpassing the representational limits of conventional DEMs. Additionally, a landscape-pattern-based visualization strategy enables spatially adaptive LOD rendering and supports semantic terrain interpretation. This framework lays the foundation for terrain simplification and efficient 3D visualization, as elaborated in subsequent sections.

1.2 Experimental Data

This paper combines multi-source remote sensing coastline constraints with the EOT20 tidal model to construct a spatiotemporal fusion product of the digital elevation model (DEM) of the Radiation Sand Ridge Group from 2019 to 2021, as shown in Figure 1.

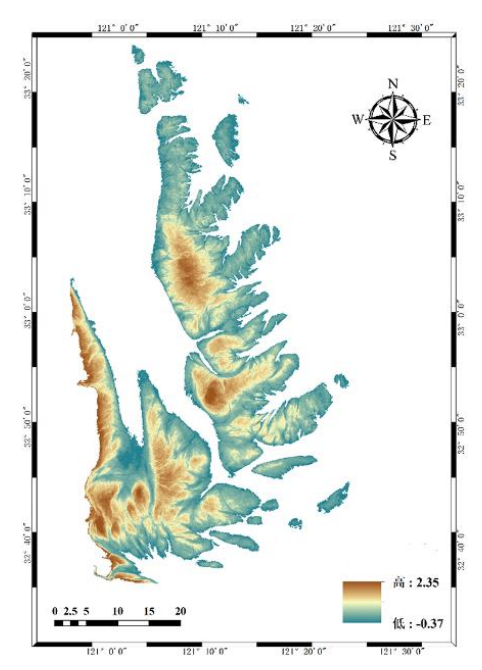


Figure 1. Three-phase DEM fusion product of the Radiation Sand Ridge Group from 2019 to 2021.

2. Methodology

2.1 Methods for constructing three-dimensional terrain models based on DEM

2.1.1 Methods for Geometric Feature Point Extraction: The key terrain feature points of the Radiating Sand Ridge Group can be categorized into geometric and semantic types. Geometric feature extraction based on DEM typically relies on indicators such as slope, curvature, undulation, and roughness. Traditional VIP algorithms using fixed global thresholds can identify features at a broad scale but fail to capture the spatial heterogeneity of the terrain. To address this, a dual-window dynamic threshold optimization model is proposed. The mean shift method determines the optimal statistical window for terrain undulation, establishing a quantitative relationship between local undulation and threshold parameters. When local terrain undulation exceeds the global average, a high-resolution detection mode is activated, applying a 3×3 window for enhanced feature extraction.

2.1.2 Methods for Semantic Feature Point Extraction: Tidal channels in the radiating sand ridge group are not only key morphological elements but also carry semantic significance linked to their formation, function, and hydrodynamic behavior. This study adopts the D8 algorithm to extract channel features from the DEM. However (Fairfield J et al., 1991), the overall flatness of the terrain—especially within tidal channels—can lead to flow direction errors and network discontinuities. To address this, a depression-filling algorithm is first applied to preprocess the DEM, ensuring flow continuity by removing local sinks within the sand ridge complex.

2.2 Multi-Scale 3D Terrain Construction Methods

2.2.1 Tidal Channel Network Classification: Constructing a tidal channel network classification system is essential for describing the multi-scale structural hierarchy of tidal channels in radiating sand ridge groups. Merely extracting the global channel framework is insufficient for tasks such as

evaluating transport capacity or calculating sediment flux. This study applies the Strahler classification method to categorize tidal channel segments (AN Quan et al.,2019) . The classification reflects channel structure and branching complexity, where higher-order channels correspond to main channels and are associated with distinct hydrological parameters, including flow velocity and discharge.

2.2.2 Multi-Scale Tidal Channel-Constrained 3D Model Simplification: This study proposes a tidal channel-constrained edge folding method (Bai H et al., 2023), combined with a quadratic error measurement-based simplification approach. During the simplification process, dynamic weight adjustment and topological constraints are applied to ensure high geometric fidelity and topological completeness in the resulting 3D terrain model. The overall workflow is illustrated in Figure 2.



Figure 2 Simplified process for tidal channel constraints

2.3 Multi-scale 3D terrain visualization method

- **2.3.1 Visualization Based on Spatially Constrained Multidimensional Clustering:** This study integrates landscape pattern indices—including total edge length (TE) and aggregation index (AI)—with spatially constrained multivariate clustering to systematically analyze the spatial distribution characteristics of the Radiating Sand Ridge Group.
- **2.3.2 Multi-Scale 3D Terrain Visualization:** This paper proposes a multi-scale visualization method that integrates geometric enhancement and semantic-driven techniques. By employing elevation exaggeration, smoothing processing, and partitioned visualization strategies, the method enhances the scientific representation and cognitive efficiency of the three-dimensional terrain of the Radiation Sand Ridge Group
- 2.3.3 3D Terrain Visualization Experiment: This study conducts a cognitive experiment on multi-scale 3D terrain visualization of the Radiating Sand Ridge Group, integrating landscape pattern indices and spatially constrained clustering. Three terrain models were compared: one without tidal channels, one with channels but no layering, and one with layered tidal channel visualization. Thirty-five geography graduate students participated in a questionnaire-based evaluation following an experimental psychology paradigm. After visual screening and consent, participants selected the model they found most effective for structural understanding. The comparison focused on clarity, readability, structural salience, and visual hierarchy. Survey results were analyzed using SPSS, and a chi-square goodness-of-fit test was applied to assess differences in model preference. Selection frequencies were also used as weights to quantify the visual cognition performance of each model.

3. Experiments and results

In this section, geometric and semantic feature points were extracted from the DEM of the Su North Radiating Sand Ridge Group. A 3D surface model was constructed based on these features, and semantic feature points were used as constraints for model simplification. A multi-level 3D terrain model was then generated according to the hierarchical structure of tidal channels and evaluated through cognitive experiments.

3.1 3D Terrain Modeling Results Based on DEM

3.1.1 Geometric Feature Point Extraction Results: This study analyzes sequential data from a moving window experiment (window sizes ranging from 2×2 to 20×20 with a step size of 1×1), as shown in Table 1. A logarithmic regression model is employed to examine the functional relationship between terrain undulation and window area, identifying the optimal window size.

Window size	Area (ten thousand m ²)	Average elevation variation /m
2×2	0.36	0.06
3×3	0.81	0.11
4×4	1.44	0.16
5×5	2.25	0.21
6×6	3.24	0.25
7×7	4.41	0.30
8×8	5.76	0.34
9×9	7.29	0.37
10×10	9.00	0.41
11×11	10.89	0.45
12×12	12.96	0.48
13×13	15.21	0.51
14×14	17.64	0.54
15×15	20.25	0.58
16×16	23.04	0.60
17×17	26.01	0.63
18×18	29.16	0.66
19×19	32.49	0.69
20×20	36.00	0.71

Table 1 Area and average terrain undulation of radiated sand ridge groups under different window sizes

Based on the data in Table 2, a quantitative relationship between average terrain undulation and statistical window area was established. A logarithmic regression model yielded a high coefficient of determination ($R^2=0.96$), indicating a strong logarithmic correlation, as shown in Figure 3(a). Second-derivative analysis further revealed a distinct unimodal pattern in the terrain variation rate curve (Figure 3(b)), peaking at the 7th point, which corresponds to a 9×9 grid window with an area of 72,900 m². Therefore, for 10 m resolution DEM data, a 9×9 grid cell is identified as the optimal statistical unit for capturing terrain undulation in the Radiating Sand Ridge Group. This window size best reflects the alternating "sandbar–tidal channel" morphology, offering a representative and accurate expression of the region's actual terrain structure.

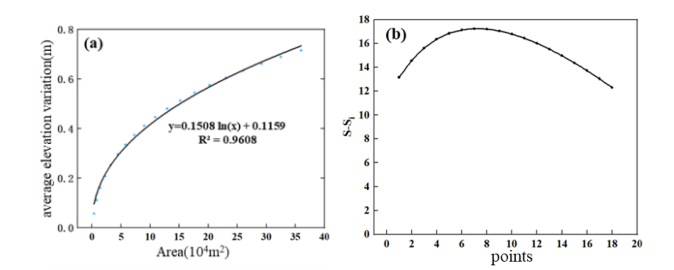


Figure 3. Determining the optimal terrain undulation window using the mean inflection point method.(a) Fitted curve of average terrain undulation versus window area;(b) S–Si variation curve based on the mean inflection point method.

This study first validates the effectiveness of constructing a 3D model using geometrically significant feature points extracted by the proposed dual-window adaptive threshold method. An internal optimization assessment highlights its advantages over conventional approaches. The method is then compared with the classical maximum Z-tolerance and traditional VIP algorithms in terms of computational efficiency, information redundancy, and geometric fidelity.

As shown in Table 2, under the same compression rate, the elevation RMSE of the resulting model is reduced to 0.34 m—an 8% improvement over the traditional VIP algorithm, 21% over the VIP with optimal windowing, and 58% over the Z-tolerance method. The dual-window adaptive threshold method effectively captures terrain heterogeneity and overcomes the limitations of fixed global thresholds, demonstrating superior performance in modeling the complex morphology of radiating sand ridge groups.

method	score	RMS E/m	MAE/m	compression ratio
VIP_3 window	114191	0.37	0.31	99.14%
VIP_9 window	113596	0.43	0.37	99.14%
VIP_double window	111457	0.34	0.29	99.16%
Maximum Z tolerance	110190	0.81	0.31	99.16%

Table 2 Comparison of model accuracy constructed using important points extracted by different algorithms

As shown in Figure 4, the three-dimensional model constructed using important geometric feature points extracted by the VIP algorithm under the dual-window adaptive threshold better reflects the spatial heterogeneity between terrain points. In contrast, the maximum Z-tolerance sampling method results in a sparser model that fails to capture the terrain characteristics of the radiating sand ridge clusters.

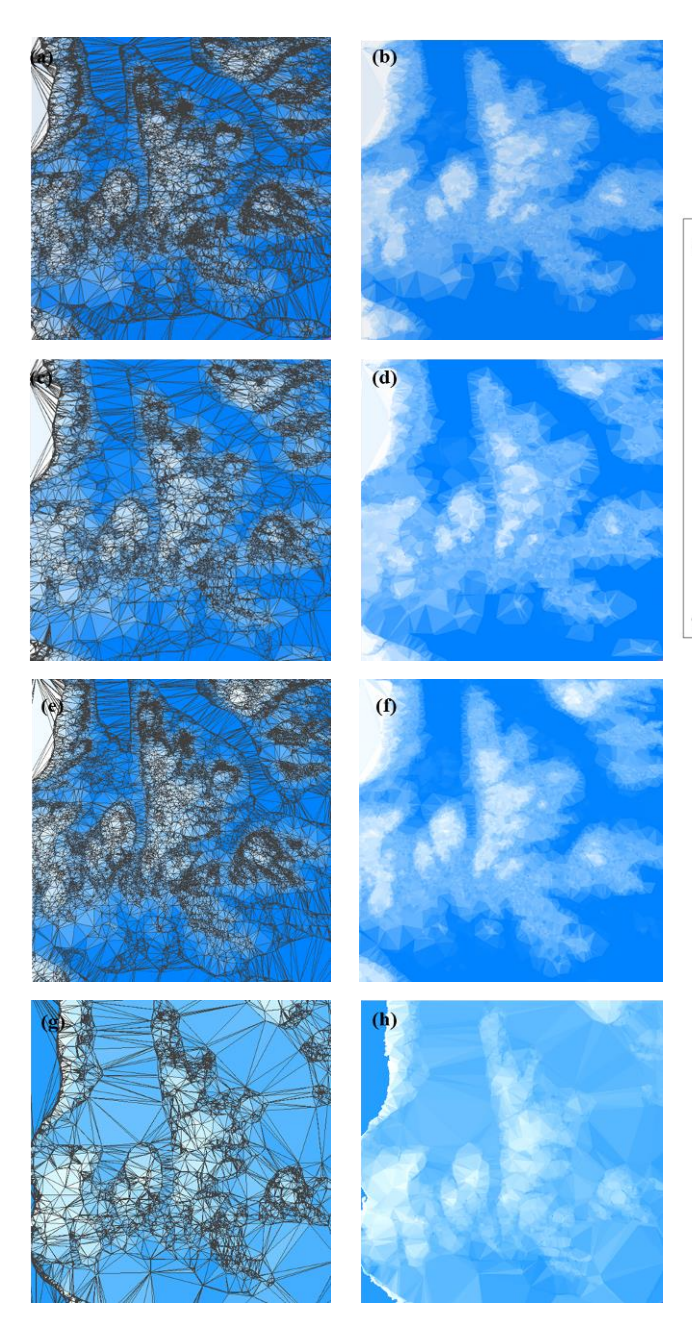


Figure 4 Comparison of three-dimensional terrain models of the Radiation Sand Ridge Group's Tiaozini Region constructed using the Maximum Z Tolerance Method and the VIP algorithm before and after improvement: (a) VIP-TIN; (b) VIP-Patch; (c) Optimal Window VIP-TI N; (d) Optimal Window VIP-Patch; (e) Dual Window VIP-TIN; (f) Dual Window VIP-Patch; (g) Maximum Z-tolerance method-TIN; (h) Maximum Z-tolerance method-patch;.

3.1.2 Results of Semantic Feature Point Extraction:

The D8 algorithm is applied to determine flow direction, followed by the calculation of cumulative flow volume. The extraction of tidal channels depends on selecting an appropriate flow threshold, which is closely related to factors such as flow velocity and channel width. In this study, the optimal threshold was determined through flow velocity experiments and applied based on the total grid count to extract tidal channels in the radiating sand ridge groups. Erroneous isolated segments were corrected using high-resolution imagery, and the resulting channels are shown in Figure 5(a). After extracting multi-level

tidal channels, the study area was subdivided into computational units (Figure 5(b)) to support spatial clustering. Semantic feature points were then generated from the hierarchical tidal channel vectors and integrated with the original geometric feature points to support enhanced terrain modeling and simplification.

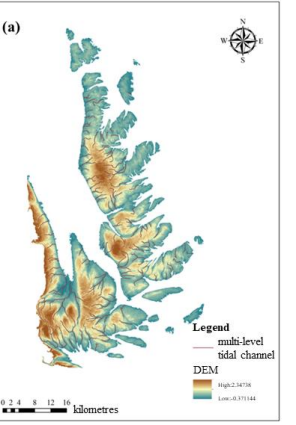




Figure 5 Multi-level tidal channel extraction and computational grid partitioning (a) Multi-level tidal channel extraction results; (b) Tidal channel computational grid

3.2 Multi-scale terrain model results

3.2.1 Results of Multi-Scale Tidal Channel Extraction in the Radiating Sand Ridge Group: Based on the tidal channel network extracted from Section 3.1.2, a hierarchical classification was performed. However, since the branching patterns of tidal channels differ from those of river systems, adjustments were necessary to the traditional tree-like hierarchical classification results. The final tidal channel hierarchical network is shown in Figure 6. In this network, higher-level tidal channels represent the main branches of the tidal channel system and exhibit macroscopic characteristics, while lower-level tidal channels represent the smaller, terminal branches and exhibit microscopic characteristics.

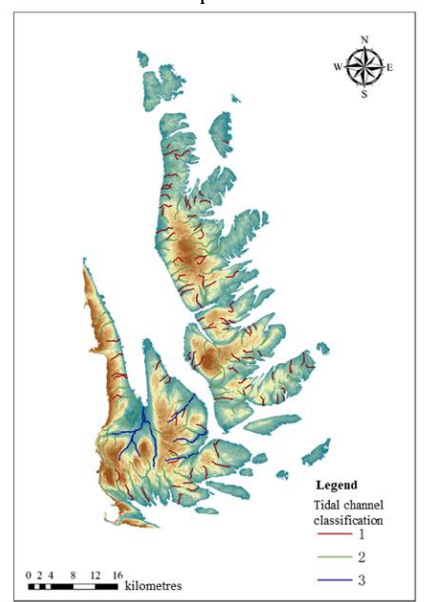


Figure 6 Multi-scale tidal channel extraction results for the Radiation Sand Ridge Group

Simplification 3.2.2 3D Terrain Results Constrained by Tidal Channels: This paper employs an incremental edge folding and QEM algorithm to construct a three-dimensional terrain model of a radiating sand ridge group constrained by multi-scale tidal channels. By setting the vertex protection weights for third-level tidal channels, terrain simplification is achieved by retaining only third-level tidal channels at different simplification rates, as shown in Figure 7. Experimental results indicate that when the simplification rate is between 50% and 87.5%, third-order tidal channels can maintain relatively complete structural features, with the maximum error stabilising between 1.72 and 7.76 m. However, when the simplification rate exceeds 87.5%, the maximum error reaches 8.92 m, and the main trunk of the tidal channel may be partially lost. Overall, the simplification algorithm based on tidal channel grade constraints can maintain certain terrain features under extremely high simplification rate conditions.

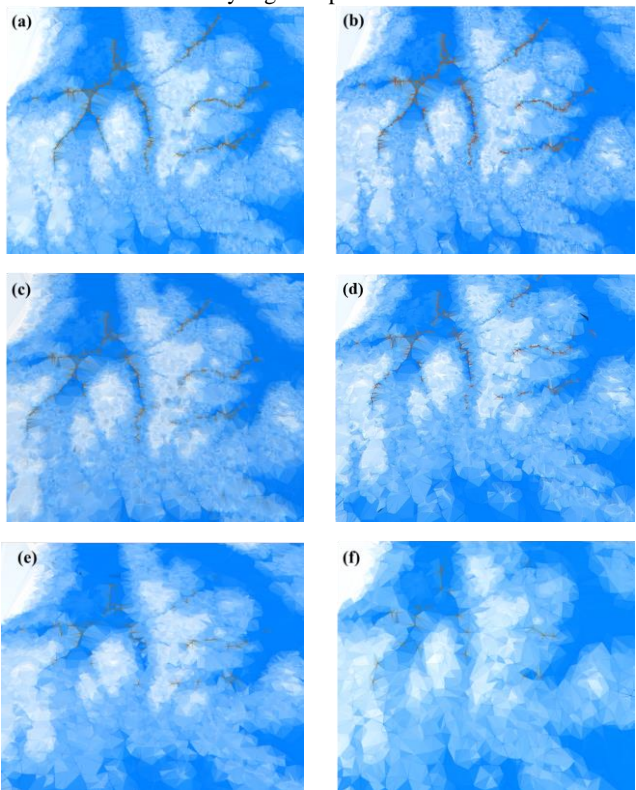


Figure 7 Three-dimensional terrain of the Radiation Sand Ridge Group in the Tiaozini area retaining third-order tidal channels at different simplification rates: (a) 50%, (b) 66.66%, (c) 75%, (d) 87.5%, (e) 93.73%, and (f) 96.86%

While retaining the complete tidal channel, this paper simplifies the model to varying degrees through progressive simplification of edge folding and the QEM algorithm to construct a multiscale terrain model. The experimental settings are as follows: the weight factor for level 3 tidal channels is 10, the weight factor for level 2 tidal channels is 2, and the weight factor for level 1 tidal channels is 0.5. The results are shown in 错误!未找到目用源。8.

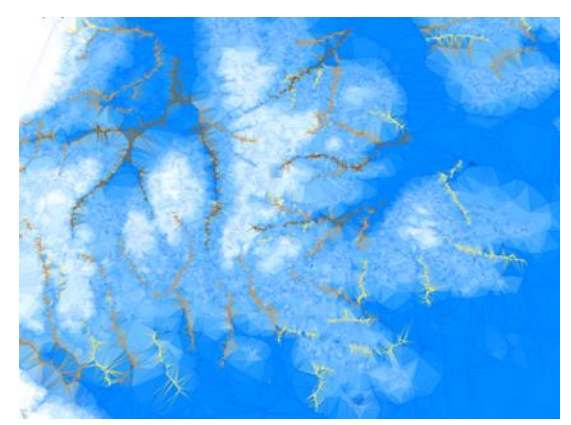


Figure 8. Locally simplified 3D terrain model of the radiating sand ridge group, preserving the tidal channel structure.

The improved 3D terrain simplification algorithm with tidal channel constraints proposed in this study integrates geometric error metrics with terrain feature awareness, ensuring both accuracy and feature fidelity in multi-scale terrain modeling. It effectively prevents structural discontinuities and preserves critical morphological elements during the simplification process.

3.3 Multi-scale 3D terrain visualisation results

Visualization Based on Spatially Constrained Multidimensional Clustering: This study applies clustering to pairwise combinations of Total Edge Length (TE) and Aggregation Index (AI) fields, as shown in Figure 9. According to the pseudo-F statistic (Figure 10), the optimal number of clusters is 22, which closely aligns with the actual spatial distribution of radiating sand ridge groups in the Tiaozini mudflat area. The combined use of AI and TE effectively suppresses over-segmentation by leveraging AI's aggregation constraint and TE's ability to distinguish shape heterogeneity. This approach accurately captures the morphological complexity of strip-like mudflats and the spatial structure of adjacent sandbanks. The resulting spatially constrained multidimensional clustering provides a reliable basis for defining large-scale visualization zones in both the Tiaozini and Dongsha areas.

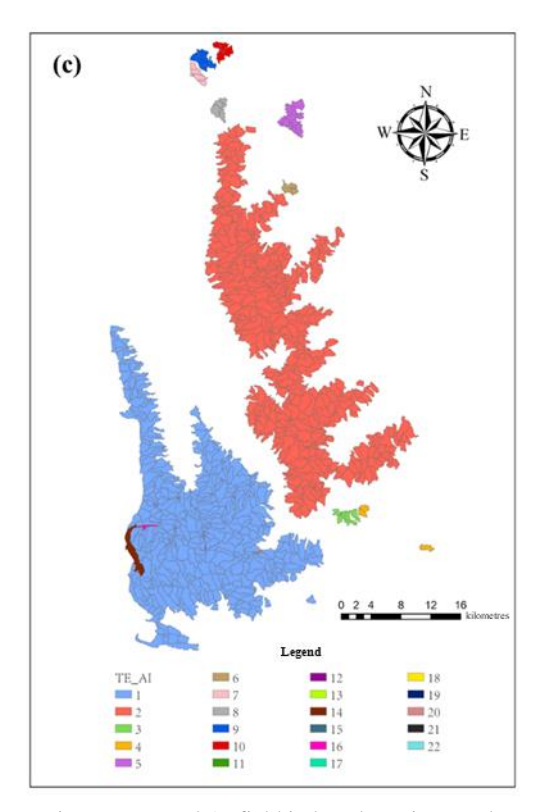


Figure 9 TE and AI field index clustering results

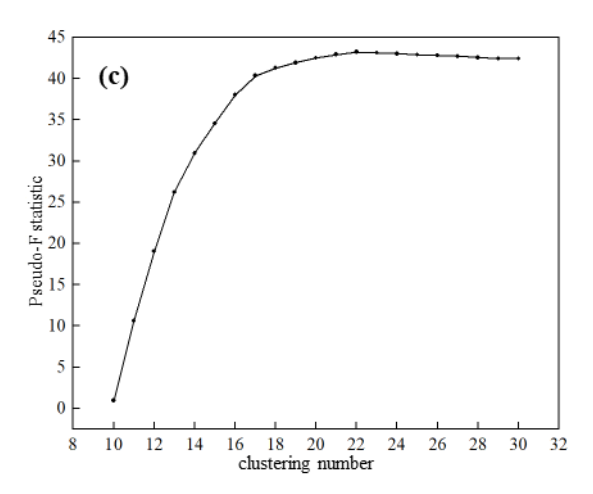


Figure 10 TE, AI field clustering pseudo-F statistic

3.3.2 Results of 3D Terrain Elevation Exaggeration: The vertical exaggeration scheme proposed in this study introduces an elevation exaggeration factor of 50×, significantly enhancing the visual recognition of key micro-geomorphic features such as sandbars, while maintaining horizontal geometric accuracy (RMSE = 5.714 m). By amplifying meter-level vertical differences into perceptible 3D morphological variations, this approach provides a new visual solution for tidal flat geomorphological analysis.

To further improve terrain quality, the 3D terrain model—constrained by tidal channels—was smoothed using a Laplacian smoothing algorithm (10 iterations). This effectively eliminated high-frequency noise and improved the clarity of both primary and secondary tidal channels, resulting in enhanced visual quality. The exaggerated and smoothed model offers robust data

support for multi-scale 3D visualization of the radiating sand ridge group.

The large-scale model retains the original, unsimplified terrain and major tidal channel structures, with blue-to-orange gradients representing elevation. The medium-scale model highlights the core area of the Tiaozini region, preserving the channel hierarchy. The small-scale model focuses on microgeomorphic units and tidal channel details. The overall results are shown in Figure 11.

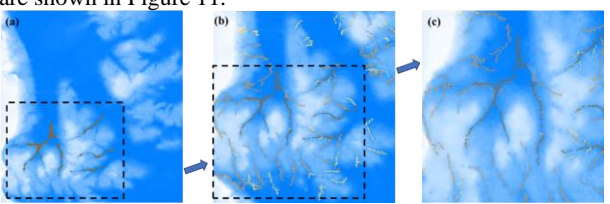


Figure 11 Three-dimensional terrain model of the radiation sand ridge group in the Tiaozi Mud area at different scales: (a) distant scale; (b) medium distance scale; (c) close distance scale.

3.3.3 Results of the 3D Terrain Visualization Cognitive Experiment for the Radiating Sand Ridge Group: This study designs four controlled experiments to evaluate the cognitive effectiveness of multi-scale tidal channel visualization, as illustrated in Figure 12.

Control Group A: 2 m-resolution remote sensing imagery of the striped mud region in the Radiating Sand Ridge Group.

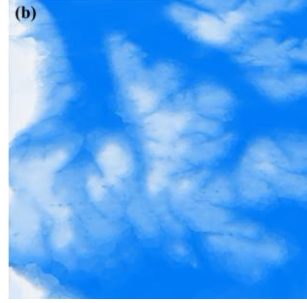
Experimental Group B: A 3D terrain model constructed using the dual-window VIP algorithm, with 50× vertical exaggeration and Laplacian smoothing. Terrain elevation is normalized and visualized using gradient shading.

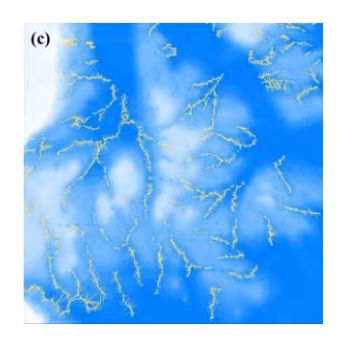
Experimental Group C: Based on Group B, this version adds unclassified tidal channel features in wireframe mode (monochrome), preserving tidal channel geometry without semantic visual encoding.

Experimental Group D: Integrates semantically classified tidal channel features with the 3D terrain and visualizes them using graded color encoding.

The base terrain in Groups B–D shares consistent parameters, including elevation range, color mapping, and viewing angle. To ensure the reliability of the cognitive assessment, the study employs a hierarchical variable control strategy to isolate the visual contributions of geometric enhancement, semantic feature retention, and semantic hierarchy in tidal channel visualization.







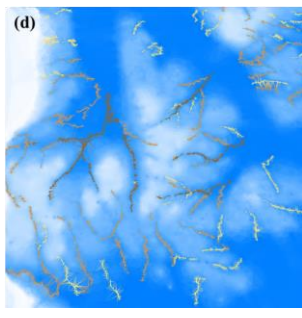


Figure 12. Visual materials for the cognitive experiment on multi-scale tidal channel visualization:(a) Control group; (b)

Experimental Group B; (c) Experimental Group C; (d)

Experimental Group D.

After collecting the Likert scale data from the completed questionnaire survey, statistical analysis will be conducted using reliability analysis, validity analysis, normality testing, analysis of variance, and post hoc multiple comparisons to validate the validity of the cognitive experiment results.

a) Reliability Analysis of Visualization Experiments for Multi-Scale Tidal Ripple Patterns in Radiating Sand Ridges: A reliability analysis was first conducted on the questionnaire data. The internal consistency of the Likert scale items (4 questions, 12 items in total) was evaluated using Cronbach's alpha. The result yielded a coefficient of 0.911 (Table 3), indicating high reliability and internal consistency of the questionnaire, and confirming the validity of the collected data.

Cronbach	Cronbach based on standardised	number
Alpha	items Alpha	of items
0.907	0.911	12

Table 3 Reliability statistics results of the multi-scale gully visualisation cognitive experiment

b) Validity Analysis of Multi-Scale Tidal Channel Visualization in the Radiating Sand Ridge Group: Next, a validity analysis was performed on the multi-scale tidal channel visualization questionnaire for the Radiating Sand Ridge Group. The KMO and Bartlett's test yielded a KMO value of 0.750 and a significance level of P<0.001 (Table 4), indicating good construct validity and that the data were suitable for factor extraction and further analysis.

KMOSampling a	0.750	
Bartlett's	approximate chi- square	413.051
sphericity test	degree of freedom	66
	significance	< 0.001

Table 4 KMO and Bartlett's test for multi-scale gully visualisation cognitive experiment

c) Normality Test for the Multi-Scale Tidal Channel Visualization Experiment in the Radiating Sand Ridge Group: Given the high reliability and validity of the questionnaire data, a normality test was conducted to assess whether the responses followed a normal distribution. The Shapiro–Wilk test (suitable for n < 50) was applied to 12 items across 4 questions, with results summarized in Table 5. Only three items—Item A (scale clarity), Item D (scale readability), and Item J (visual hierarchy)—met the normality criterion at the 5% significance level. The remaining nine items exhibited varying degrees of skewness. Specifically, Item H (scale

structural significance) showed a right-skewed distribution, while the others were left-skewed, as illustrated in Figure 13.

In summary, 3 out of 12 items conformed to a normal distribution, while 9 deviated. However, all skewness absolute values were below 1.6, suggesting that the data generally approximated a normal distribution and are acceptable for further parametric or non-parametric analysis.

dimension	annotation	model	Shapiro- Wilk pvalue	Conclusions at the (5%) level
clarity	A	В	0.227	normal
clarity	В	C	0.009	non-normal
clarity	C	D	< 0.001	non-normal
readability	D	В	0.141	normal
readability	Е	C	< 0.001	non-normal
readability	F	D	< 0.001	non-normal
structural significance	G	В	0.022	non-normal
structural significance	Н	C	0.005	non-normal
structural significance	I	D	< 0.001	non-normal
Visual hierarchy	J	В	0.162	normal
Visual hierarchy	K	С	0.038	non-normal
Visual hierarchy	L	D	< 0.001	non-normal

Table 5 Multi-scale gully visualisation data grouping and Shapiro-Wilk test results

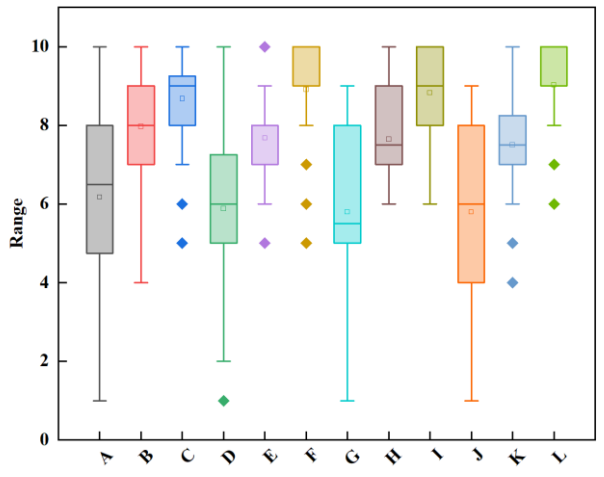


Figure 13 Statistical distribution of data for each item in the questionnaire scale

d) ANOVA and Post Hoc Comparison of Multi-Scale Tidal Channel Visualization in the Radiating Sand Ridge Group: Analysis of variance (ANOVA) was employed to assess whether significant differences existed among the four experimental groups across four dimensions of visual perception. Given that the original data were approximately normally distributed and that the same participants evaluated all models, the data followed a repeated measures design. Due to heteroscedasticity confirmed by Levene's test, Welch's ANOVA was applied. Results indicated statistically significant differences (p < 0.05) across all four dimensions—clarity, readability, structural distinctiveness, and visual hierarchy—among the four groups of radiating sand ridge models.

Post hoc analysis using the Games–Howell test revealed that, in terms of clarity (Figure 14a), both the ungraded tidal channel terrain (Group C) and the multi-scale graded channel model (Group D) scored significantly higher than the patch-pattern terrain (Group B). This demonstrates that incorporating visible tidal channel networks and multi-scale classification enhances the discernibility of geomorphic structures.

For readability, structural distinctiveness, and visual hierarchy (Figures 14b–d), Group D consistently achieved the highest scores, followed by Group C, while Group B scored the lowest. This confirms that visualizing multi-scale tidal channel features significantly improves cognitive perception. At the macro scale, Laplacian smoothing reduced surface noise and enhanced overall readability. At the micro scale, hydrology-driven morphological enhancement of ripple boundaries further improved structural recognition and terrain clarity.

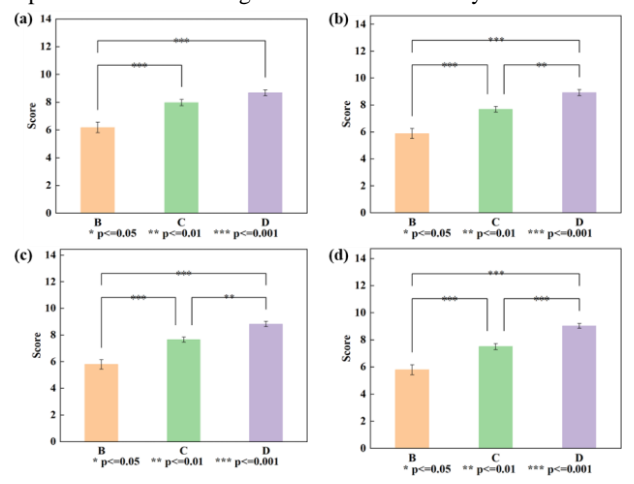


Figure 14 Data differences between different 3D terrains (a) clarity; (b) readability; (c) structural significance; (d) visual hierarchy

As shown in Figure 15, radar chart analysis across the four evaluation dimensions—clarity, readability, structural significance, and visual hierarchy—reveals that the original 3D terrain performed the worst. The 3D terrain constrained by tidal channels showed moderate performance, while the multi-scale tidal channel-constrained terrain of the radiating sand ridge group achieved the highest scores across all dimensions, demonstrating superior visual and structural interpretability.

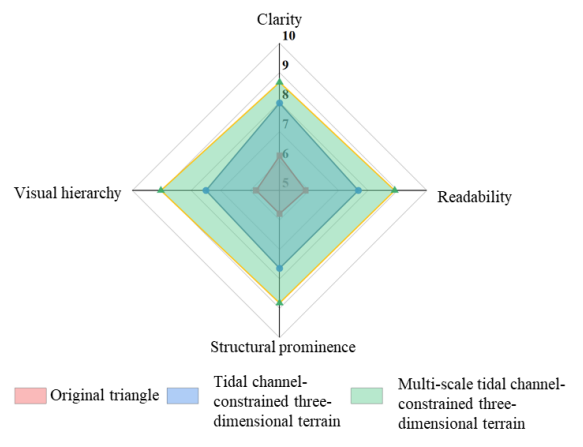


Figure 15 Scores for four dimensions between different threedimensional terrains

The questionnaire results demonstrate that the 3D terrain model of the Radiating Sand Ridge Group, constrained by multi-scale tidal channels, effectively integrates macro-terrain representation with detailed micro-channel features. It achieved the highest scores in clarity, readability, structural significance, and visual hierarchy, significantly enhancing users' cognitive perception. These findings confirm the effectiveness of the proposed method from a user experience perspective, validating its applicability for multi-scale geomorphic visualization and interpretation.

4. Conclusion

This study explores 3D terrain modeling and visualization methods for multi-scale radiating sand ridge groups, establishing a terrain visualization framework constrained by geometric and semantic features. Theoretically, it introduces the mean variable point method and terrain undulation analysis into the window selection process of the traditional VIP algorithm, addressing the limitations of manual window configuration. Methodologically, it proposes a novel 3D terrain simplification approach constrained by tidal channel semantics, achieving a balance between feature preservation and computational efficiency. Finally, cognitive experiments confirm the effectiveness of ripple ridge-constrained visualization in enhancing spatial cognition, providing a scientific foundation for improved terrain modeling and visual analysis of complex coastal geomorphology.

Acknowledgements

This work was supported by the National Natural Science Foundation of China (Grant Nos.42471488, 42371397, and 42371443), the Marine Science and Technology Innovation Project of Jiangsu Province (Grant No. JSZRHYK202302) and the Open Fund of Key Laboratory of UrbanLand Resources Monitoring and Simulation, Ministry of Natural Resources (Grant No. KF-2023.08-20).

References

An, Q., He, Z., & Zhao, C. (2019). GIS-based estimation of fractal dimension and geomorphological development of the water system in the dam construction area. *Remote Sensing for Natural Resources*, 31(4), 104–111. (in Chinese)

Bai, H., Shen, T., Huo, L., et al. (2023). Improved edge folding algorithm for 3D building models taking into account the visual features. *Buildings*, *13*(11), 2739.

Du, Y. (2005). A research on key technologies for global multiresolution virtual terrain environment (PhD dissertation, PLA Information Engineering University). 173 pp. (in Chinese)

Fairfield, J., & Leymarie, P. (1991). Drainage networks from grid digital elevation models. *Water Resources Research*, 27(5), 709–717.

Gu, Y., Zhang, Y., & Liu, Y. (2010). Remote sensing technology in measurement and analysis on the topography evolution of the radial sand ridges in South Yellow Sea. In *Proceedings of the 2nd Conference on Environmental Science and Information Application Technology* (Vol. 1, pp. 849–853). IEEE.

- Hoppe, H., DeRose, T., Duchamp, T., et al. (1993). Mesh optimization. In *Proceedings of the 20th Annual Conference on Computer Graphics and Interactive Techniques* (pp. 19–26).
- He, H., Zhang, N., & Liu, H. (2005). Stability of major tidal channels in the radial submarine sand ridge system off Jiangsu Province. *Marine Sciences*, 29(1), 12–16. (in Chinese)

Wang, Y., Zhu, D., You, K., et al. (1999). Evolution of the radiative sand ridge field of the South Yellow Sea and its sedimentary characteristics. *Science in China Series D: Earth Sciences*, 42, 97–112.